INFLUENCE OF CHEMICAL STRUCTURE ON THE FLUIDITY OF RAPIDLY HEATED BITUMINOUS VITRINITES

Jonathan P. Mathews, Patrick G. Hatcher, Alan W. Scaroni
Energy & Fuels Research Center and Fuel Science Program, 211 CUL, The Pennsylvania State University, University Park PA 16802

Keywords: Vitrinite, char morphology and thermoplastic transformations.

ABSTRACT
When heated rapidly, many coal particles undergo thermoplastic transformations which change the particle size, shape and morphology. In the current work, vitrinites with subtle differences in rank and bulk chemical composition but significant differences in chemical constitution produced chars with different particle size and helium density. The particle size of an Upper Freeport (UF) sample increased by a factor of 2.5, and the helium density increased to 2.1 g/cm^3 (daf). In contrast, a Lewiston-Stockton (LS) vitrinite swelled by a factor of 1.8 and the helium density increased slightly then decreased to 1.3 g/cm^3. The LS vitrinite had more aliphatic hydrogen than the UF vitrinite, which should promote thermoplasticity. However, less aromatic hydrogen and more oxygen in the LS sample contributed to increased "cross-linking", presumably increasing the lamella size in the thermoplast, thus reducing the extent of thermoplasticity.

INTRODUCTION
Much of the published work on the properties of chars produced from coals that have undergone thermoplastic transformations has been with whole coals. However, macerals have different extents of thermoplasticity, hence by using whole coals individual maceral behaviour has been masked (1-3). While new separation techniques produce maceral concentrates (4), the associated particle size is typically less than pulverised coal. Although similar in rank and bulk chemical composition, two Illinois No. 6 coal samples were found to develop different extents of thermoplasticity during rapid heating (5). Since maceral analyses were not reported, fluidity differences manifested as different char properties might be explained by differences in the maceral composition. A relationship between chemical structure (total aliphatic hydrogen) and a modified Giesler fluidity has been reported for vitrinites, with an abrupt increase in fluidity over a relatively narrow range of aliphatic hydrogen (6). Furthermore, it has been proposed that three criteria must be met for plasticity to occur in bituminous vitrinites: 1) the presence of lamellae-bridging structures that can be thermally ruptured, 2) a supply of hydroaromatic hydrogen and 3) an initial, intrinsic potential for micellar and lamella mobility (not related to the rupture of chemical bonds), which provides opportunity for the free-radicals formed by bond rupture to contact potentially transferable hydrogen (7). Thus, the relationship between thermoplastic behaviour and chemical constitution can be explored utilizing vitrinites of subtly different bulk composition but different chemical constitution. In this study, particle swelling and helium density of the resulting chars were measured and related to differences in the vitrinite chemical structure.

EXPERIMENTAL
The vitrain samples were collected from *Sigillaria* (a type of Lycopod) tree remains in the roofs of coal mines in the Upper Freeport (UF) and Lewiston-Stockton (LS) coal seams. The samples were comminuted in a Holmes 501XLS pulveriser. A narrow particle size separation was achieved by wet sieving with a series of (U.S. Standard) sieves. Char particles were collected after rapid heating to 1500°C in a drop-tube reactor similar to that discussed previously (8). Coal was fed by an Acrison GMC-60 feeder through a water-cooled injector at a rate of 0.33g/min and entrained by 1.0 L/min of primary nitrogen. The tip of the injector was level with the bottom of a mullite flow-straightener. Secondary nitrogen (3.0 L/min) was preheated to 830 °C and exited the flow straightener with the primary nitrogen. Char particles were collected using a water-cooled probe with a cold suction flow of 4.0 L/min. Char particles were obtained from various locations by raising and lowering the collection probe.

The particle size distributions of vitrinite and collected vitrinite-chars were determined with a laser light scattering instrument (9). Helium densities were obtained using a commercially-available pycnometer. Changes in the morphology of the char were followed using gold-coated samples in a SEM. Ultimate analyses were performed using commercially-available instrumentation. Proximate analyses were determined using a thermogravametric analyser (5 mg sample size) utilizing a modified ASTM methodology (10). The mean maximum vitrinite reflectance was calculated in accordance with ASTM procedures (11). CPMAS ^{13}C NMR and dipolar dephasing experiments were performed in ways similar to those reported previously (12).

RESULTS AND DISCUSSION

The mean maximum vitrinite reflectance values were 0.97 (sd 0.04) and 0.93 (sd 0.08) for the UF and LS vitrinites, respectively. Both samples were determined to be monomaceral in composition using polished briquettes with reflected white and blue light. The elemental compositions of the vitrinites normalized to 100 carbon atoms were $C_{100}H_{75.5}N_{1.2}O_{4.4}S_{0.0}$ and $C_{100}H_{77.9}N_{1.4}O_{6.3}S_{0.6}$ (oxygen determined by difference) for the UF and LS vitrinites, respectively. The elemental compositions differed subtly, however in that, the LS vitrinite was slightly richer in hydrogen, nitrogen, sulphur and oxygen. Aromaticities determined by ^{13}C NMR were 0.77 and 0.81 for the UF and LS vitrinites, respectively (Table 1). Thus, the vitrinites were of the same maceral composition, with close particle size distributions (Table 2), yet subtle differences in the rank (mean maximum vitrinite reflectance) and aromaticities (Table 1). The volatile matter (daf basis) for the 200x400 mesh cuts were 37 and 30% for the UF and demineralized LS vitrinites, respectively. This indicates that, although there were only subtle differences in the bulk chemical composition, the constitution of the two vitrinites was substantially different. Structural parameters derived from the elemental composition and ^{13}C NMR experiments are reported in Table 1. The LS sample was richer in total aliphatic hydrogen (H/Cali) in comparison to the UF vitrinite and had less aromatic bound hydrogen. The lower aromatic hydrogen and higher oxygen content are consistent with a more "cross-linked" structure for the LS vitrinite.

SEM micrographs of the wet sieved 200x400 mesh UF and LS vitrinites and drop-tube generated vitrinite-char particles are presented in Figure 1. The UF vitrinite and chars are shown at different magnifications to aid in following morphological changes. The LS vitrinite and vitrinite-chars are shown at the same magnification to allow visual representation of the swelling. The wet sieved vitrinite fraction for both samples was characterized by angular particles with generally sharp edges. The char particles collected at 13 cm showed that some of the UF particles had undergone thermoplastic transformations, resulting in the rounding of edges and occasional cenosphere formation. However, many of the particles retained their angular shape and sharp edges. In contrast, most of the LS vitrinite chars at the 13 cm sampling location remained angular. The light-scattering-obtained volumetric weighted average size ($D[v,0.5]$) indicated little swelling for both samples at the 13 cm location (Table 2).

The vitrinite-char particles for both samples collected at the 23 cm location displayed the characteristics of greater fluidity, in that very few particles retained their original morphologies and there was a slight increase in the $D[v,0.5]$ (Table 2). The char particles collected at the 33 cm location had increased in size, swelling by a factor of 2.5 for UF vitrinite chars with the distribution of particle sizes increasing by a factor of 3.9 as shown by the Δ value (the difference between the $D[v,0.9]$ and $D[v,0.1]$ diameters). In contrast, the LS vitrinite-chars were less swollen, only expanding by a factor of 1.8 with the Δ value increasing by a factor of 1.6. As both vitrinite particle size cuts had similar Δ's, indicating similar particle size distributions, the swelling of the UF sample was more sensitive to particle size. For both samples the char particles were almost all cenospheres. The outer skins of the cenospheres appeared wrinkled in many cases, which may be indicative of contraction. Decreasing $D[v,0.5]$ values for both samples after the 33 cm location supports the occurrence of contraction. It might be expected that contraction would occur immediately after the jet release phenomenon (13), where the internal pressure is released suddenly and violently. However, cenospheres collected at the 23 cm location contained rents and blowholes, indicative of a sudden jet-release of volatiles, yet the skins remained smooth. Thus, contraction appears to post-date the jet-release event. It is speculated that the contraction of the particles may therefore be linked to chemical changes affecting fluidity rather than physical changes affecting the internal pressure (3). The cenospheres collected at the 33 cm location contained soot agglomerates on their skins. Chars collected at the 43 and 53 cm locations (not shown) were thin walled, having undergone some structural collapse.

Helium densities for the demineralized vitrinites and vitrinite-chars for both samples are shown in Figure 2, and compared to the reported density of graphite (14). The UF vitrinite chars showed a slight increase in helium density with increasing reactor length until after the 23 cm location where a substantial increase in the helium density occurred. In contrast, the LS vitrinite-chars experienced a slight increase in helium density (at the 13 cm location) and then a decrease to 1.3 g/cm^3. A lower helium density is consistent with the observed reduced thermoplasticity of the LS vitrinite.

CONCLUSIONS

Two vitrinites with only subtle differences in bulk chemical composition exhibited different extents of thermoplastic transformations upon rapid heating as manifested by particle swelling and the helium densities of the resulting chars. The Lewiston-Stockton sample, although richer in total aliphatic hydrogen, did not experience enhanced thermoplastic transformations in comparison to the Upper Freeport vitrinite. The higher concentration of oxygen and less aromatic hydrogen in the Lewiston-Stockton vitrinite are consistent with a more cross-linked structure. This appears to reduce the fluidity, presumably by increasing the size of the lamellae, and produced chars with lower helium density and smaller particle size in comparison to the UF vitrinite.

REFERENCES

1. Tsai, C.-Y. and Scaroni, A. W., *Fuel*, 1987, **66**, (2), 200.
2. Street, P. J., Weight, R. P. and Lightman, P., *Fuel*, 1969, **48**, 343.
3. Anson, D., Moles, F. D. and Street, P. J., *Combustion & Flame*, 1971, **16**, 265.
4. Taulbee, D., Poe, S. H., Robl, T. and Keogh, B., *Energy & Fuels*, 1989, **3**, 662.
5. Cai, M. F., Guell, A. J., Dugwell, D. R. and Kandiyoti, R., *Fuel*, 1993, **72**, (3), 321.
6. Senftle, J. T., Kuehn, D. W., Davis, A., Brozoski, B., Rhoads, C. and Painter, P. C., *Fuel*, 1984, **63**, (2), 245.
7. Neavel, R. C., Coal Agglomeration and Conversion, West Virginia Geological and Economic Survey, 1975, Morgantown, WV. 120.
8. Artos, V. and Scaroni, A. W., *Fuel*, 1993, **72**, (7), 927.
9. Allen, T., Particle size measurement, Vol 4, 1990, London, Chapman and Hall.
10. ASTM, Designation: D 5142 - 90, Standard test methods for proximate analysis of the analysis sample of coal and coke by instrumental procedures, in Annual book of ASTM standards, Section 5, Petroleum products, lubricants and fossil fuels, 1994, 442.
11. ASTM, Standard test method for microscopical determination of the reflectance of vitrinite in a polished specimen of coal, in Annual book of ASTM standards, Section 5, Petroleum products, lubricants and fossil fuels, 1995, 274.
12. Hatcher, P. G., *Energy & Fuels*, 1988, **2**, 40.
13. Grey, V. R., *Fuel*, 1988, **67**, (9), 1298.
14. Franklin, R. E., *Fuel*, 1948, **27**, (1), 46.

Table 1. Chemical parameters

Parameter	UF	LS
f_a (CPMAS)	0.77	0.82
aryl-O content	0.20	0.17
$f_a^{a,H}$	0.49	0.37
H/C	0.76	0.78
H/Cali	1.7	2.7

f_a is the aromaticity, aryl-O content is the ratio of aryl-O bonded carbons to total aromatic carbons, $f_a^{a,H}$ is the fraction of aromatic carbons that are protonated, H/C is the atomic hydrogen to carbon ratio, H/Cali is the aliphatic atomic hydrogen to carbon ratio.

Table 2. Particle size distribution for the vitrinite and vitrinite-chars

Sampling Location (cm)	$D[v,0.5]$ μm	$D[v,0.9]$ μm	$D[v,0.1]$ μm	Δ μm	Swelling
Vitrinite (UF)	65	110	44	66	1.0
13	69	120	48	72	1.1
23	76	132	48	86	1.2
33	160	298	42	255	2.5
43	148	223	54	169	2.3
53	132	210	59	151	2.0
Vitrinite (LS)	61	92	39	53	1.0
13	75	106	49	57	1.2
23	76	139	46	93	1.2
33	109	191	55	136	1.8
43	103	185	49	136	1.7

Analysis is based on volume, $D[v,0.5]$ is the volumetric weighted average size. $D[v,0.90]$ is the particle diameter such that 90% of the total volume is in particles of smaller diameter. $D[v,0.1]$ is the particle diameter such that 10% of the total volume is in particles of smaller diameter, Δ is the difference between the $D[v,0.90]$ and $D[v,0.1]$ diameters, swelling was calculated from the $D[v,0.5]$ diameter, particles were assumed to be spherical and no shape correction was performed. Data were collected in the model independent mode.

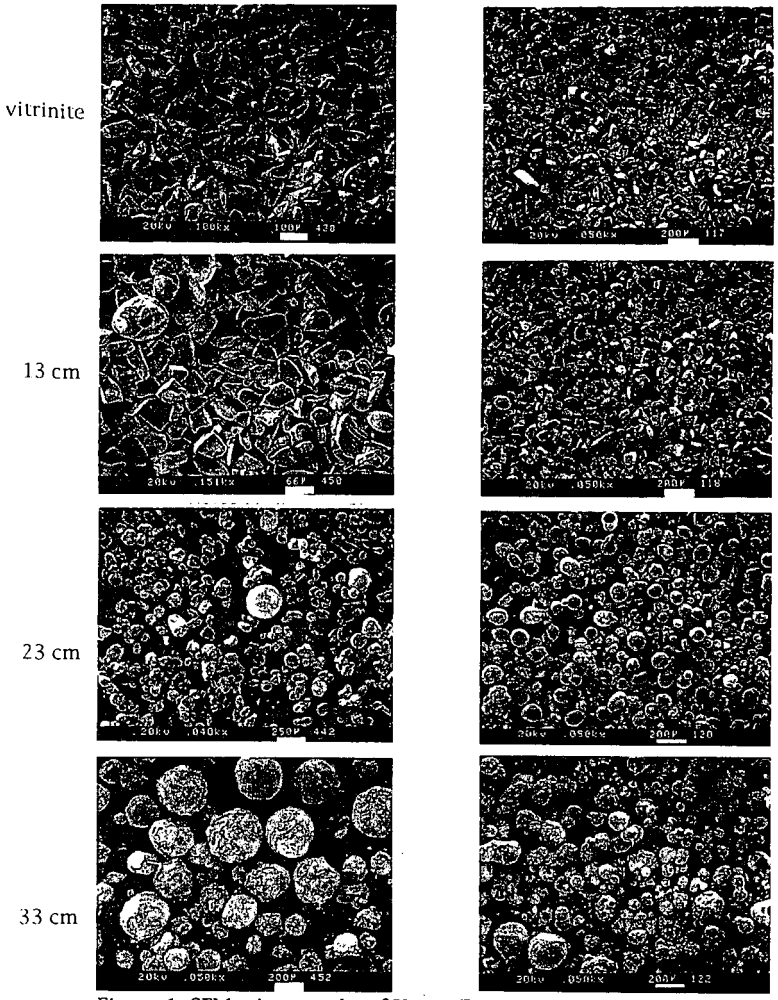

Figure 1. SEM micrographs of Upper Freeport (left) and Lewiston-Stockton (right) vitrinite and vitrinite-chars.

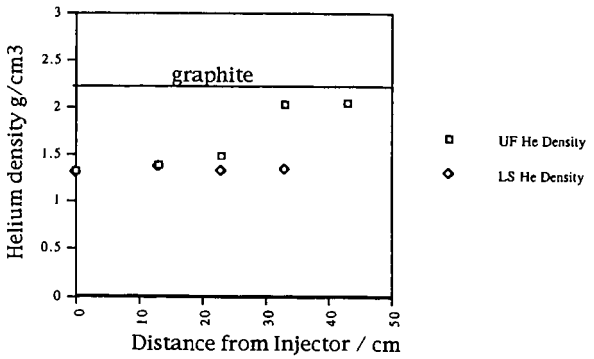

Figure 2. Helium densities for demineralized UF and LS vitrinites and vitrinite-chars